

## Possibility of the Existence of Non-Carbon Fullerenes: Ab Initio HF and DFT/B3LYP Studies of the IV Main Group Fullerene-Like Species

Jerzy Leszczynski\* and Ilya Yanov

The Computational Center for Molecular Structure and Interactions (CCMSI), Department of Chemistry, Jackson State University, Jackson, Mississippi 39217-0510

Received: May 15, 1998; In Final Form: September 30, 1998

A comprehensive investigation of the equilibrium geometries, cohesive energies, and electronic properties of the IV main group fullerene-like compounds  $C_{60}$ ,  $Si_{60}$ ,  $Ge_{60}$ ,  $Sn_{60}$ , and  $Pb_{60}$ , has been performed by ab initio molecular modeling at the HF/Lan11DZ and B3LYP/Lan11DZ levels. In addition, the effect of the basis set on the structure and properties of  $C_{60}$  and  $Si_{60}$  has been examined at the STO-3G, Lan11DZ, and 6-31G(d) levels. Our calculations confirmed the possibility of the existence of these species. It was found that the values of the relative bond alternation, cohesive energy, HOMO–LUMO gap, and the ionization potential of the molecules decrease monotonically in going down the IVth group from  $C_{60}$  to  $Pb_{60}$ . The obtained data for  $Ge_{60}$  is rather similar to the one for  $Si_{60}$ , and also the molecular parameters for  $Sn_{60}$  are close to the appropriate values both for  $Si_{60}$  and  $Ge_{60}$ .

### Introduction

The discovery of carbon molecules with geodesic structures has prompted a number of studies, both theoretical and experimental, on the possible existence of non-carbon analogues of these species.<sup>1,a,b,2,3</sup> From a theoretical point of view it opens the way toward the preparation of new forms of known substances. Besides theoretical interests, such polyhedrons will facilitate a much more diverse chemistry than has been possible so far with carbon fullerenes. It is quite possible that the unique properties of geodesic structures will find utilization in future nanotechnology.

In spite of the repeated recognition of fullerene-like polymorphs<sup>4–6</sup> it has so far been impossible to isolate them in amounts comparable to those obtained for  $C_{60}$  and  $C_{70}$ . Therefore the experimental study of such systems is quite difficult. As a promising alternative, computer simulations are able to furnish reliable data concerning geometries and stabilities of non-carbon fullerenes.

Our work is devoted to the ab initio study of the series of IV main group fullerene-like compounds:  $C_{60}$ ,  $Si_{60}$ ,  $Ge_{60}$ ,  $Sn_{60}$ , and  $Pb_{60}$ . To gain insight into the existence and formation paths of such structures, we will compare their properties predicted at the common level of theory.

There are only a few studies devoted to the fullerene-like structures, based on elements distinct from carbon or silicon.<sup>7–9</sup> The majority of investigations related to non-carbon clusters have been performed on silicon systems, perhaps because of silicon's applications in the microelectronic industry. Following is a comprehensive review of the structures, formation process, and physical–chemical properties of these species.

### Background

**Mass Spectrum Data.** Now it is generally accepted that there are three distinct regions characterizing the carbon clusters mass spectrum:<sup>10</sup> (1) the small clusters, containing fewer than 25 atoms, consisting of chains and monocyclic rings; (2) a region

between about 20 and 35 atoms in which species of any sort were observed; and (3) an even-numbered cluster distribution from the high 30's to well over 150 atoms.

In contrast to experiments with  $C_N$  or alkali $_N$  compounds, the abundance spectra of  $Si_N$  do not display the signatures of the magic numbers.<sup>11</sup> However, observation of  $Si_N$  ( $10 < N < 100$ ) reveals a very remarkable size selectivity of  $Si_N$  clusters. In a series of pioneering measurements, Smalley and co-workers studied the reactivity of these clusters with ammonia.<sup>12</sup> Making admission for chemisorption of ammonia yields reactivity minima for  $Si_N$  clusters with  $N = 21, 23, 39, 45$  indicating a particularly high degree of saturation, corresponding to preferred geometric shapes for these “magic” counts of constituents. As a common finding from all these measurements,  $Si_N$  clusters exhibit strong reactivity oscillation with size in the region  $N \leq 47$ . For larger systems, the dependence of reactivity on size has turned out to be rather smooth.

A crucial experimental result concerning the shapes of  $Si_N$  was obtained by Jarrold et al.<sup>13</sup> Investigating the mobilities of size-selected  $Si_N$  cluster ions in a helium atmosphere the authors conclude that the  $Si_N$  geometries undergo a transition around  $N = 27$  from prolate to quasi-spherical shapes. Photoionization spectra<sup>14</sup> reveal similar features for the clusters in the size range  $18 \leq N \leq 41$ , hinting at the possibility of a common bonding network for mid-sized  $Si_N$  clusters.

A comparison of the carbon and silicon compounds indicates that there is no favorable even-numbered distribution of silicon clusters, but there is a tendency for the clusters to form quasi-spherical shapes. The  $Si_N$  clusters differ significantly from the corresponding  $C_N$  species since there is no evidence for linear or cap structures for the silicon compounds.

**Fullerene Formation Mechanism.** A common technique of the macroscopic generation of fullerenes is the arc-discharge method under controlled pressure of inert gas proposed by Haufler et al.<sup>15</sup> Usually the generated fullerenes consist of 80%  $C_{60}$ , 15%  $C_{70}$ , and a small amount of the higher fullerenes.

In spite of a number of serious investigations, the formation mechanism of fullerenes is not clear. Several models have been

\* Corresponding author.

proposed on the basis of experimental insights (see, for example, the detailed review of Yamaguchi and Maruyama<sup>16</sup>). Haufler et al.<sup>15</sup> conclude that the growth of a hexagonal network is the result of additions of carbon dimers and trimers. They state that the pentagons are essential for curvature and for decreasing the number of dangling bonds. On the other hand, the interaction between two neighboring pentagons should result in too high strain on the network system, so the “isolated pentagon rule” was assumed. Quite different precursors to the fullerene structure were proposed such as a piece of a graphite sheet<sup>17</sup> or a bucky tube.<sup>18</sup> Alternately, Heath<sup>19</sup> proposes a model for the clustering sequence in which there is a linear chain up to C<sub>10</sub>, rings in the C<sub>10</sub>–C<sub>20</sub> range, and a fullerene-type structure for C<sub>30</sub>. He claims that successive C<sub>2</sub> additions follow until the isolated pentagon rule is satisfied. Recently, the drift tube ion chromatography experiments of laser-vaporized carbon clusters show the existence of polycyclic rings and the possibility of annealing such a structure to a fullerene.<sup>20</sup>

The main similarity among the proposed models is the concept that flat or cap polycyclic species are considered as precursors. It is also of interest that both fullerenes and closed-shell silicon clusters are not the global minimum energy species under formation conditions and probably in the whole phase diagram,<sup>21</sup> so the formation process of these compounds must be kinetically controlled.

**Quantum-Chemical Calculations.** A series of ab initio quantum-chemical computations have been performed on Si<sub>N</sub> systems. Si clusters in the size range 3 < N < 15 have been investigated by the Hartree–Fock and MP2 methods.<sup>22</sup> The tendency of such clusters toward the deformation of the original geodesic shell structures into configurations of lower symmetry which are composed of a negatively charged “core” and a positively charged “shell” is revealed. The energy difference between cage-like and ground-state structures diminishes as one goes from N = 4 to N = 8, and the cohesive energy rises to a maximum for Si<sub>10</sub>. From this observation, one may infer that small Si<sub>N</sub> clusters with N = 4, 6, 8, 10 tend to adopt the cage-like structures as N increases.

Intermediate-sized Si clusters, containing 20 to 33 atoms, have been studied using the first-principles methods based on the local density approximation.<sup>23</sup> The calculations reveal the complex relationships between the properties of the clusters and the cluster structures. The authors studied three classes of structures over the entire size range, including elongated structures formed by stacking a basic structural unit along a common axis, compact structures which attempt to minimize the cluster surface area, and single-shell fullerene structures. They found evidence suggesting a transition in stability from the elongated structures to the compact structures at a cluster size of N = 26 atoms which is in good agreement with experimental results. The stability of the fullerene structures is intermediate over the whole size range studied. Therefore, the closed-shell silicon clusters, like fullerenes, do not necessarily prefer the most compact geometric arrangement, and the fullerene structures are intermediate in energy among the considered systems.

A number of theoretical studies has been devoted to the possible existence of the Si<sub>60</sub> fullerene. It was concluded that the difference in total energy (HF/DZ+ECP) between the octahedral Si<sub>24</sub> and Si<sub>60</sub> clusters per silicon atom is 10.3 kcal/mol in favor of Si<sub>60</sub>.<sup>3</sup> This value approximately amounts to half of the corresponding value of 22.3 kcal/mol calculated for C<sub>60</sub> using the HF/STO-3G method.<sup>24</sup> As a result of the larger bond distances, Si<sub>60</sub> has a hollow cage bigger than that of C<sub>60</sub>. Bond orders of 1.078 and 1.101 (1.681 and 1.495) are obtained from

AM1 calculations<sup>2</sup> for pentagonal bonds (hexagonal bonds) of Si<sub>60</sub> and C<sub>60</sub>, respectively. Therefore, the loss of delocalization in passing from C<sub>60</sub> to Si<sub>60</sub> is shown.<sup>2</sup>

The calculated electronic structure of Si<sub>60</sub> indicates<sup>2</sup> that the highest occupied molecular orbital and the lowest unoccupied molecular orbital display the same symmetry as those of C<sub>60</sub> and that the HOMO–LUMO gap is approximately half as large as that for C<sub>60</sub>. As predicted for smaller size clusters, the geodesic form is not the most stable structure of Si<sub>60</sub>.<sup>25</sup>

In summary, on the basis of the available experimental and theoretical data, neither the existence nor the nonexistence of non-carbon fullerene polymorphs can be concluded. However, since sp<sup>2</sup> bonding is energetically more favorable for C<sub>N</sub> than for Si<sub>N</sub>, in the latter there are no caps and no plane structures which play a crucial role in fullerene formation. It seems that the mechanism of formation of such complexes is different. Taking into account the fact that the fullerene structure is not the global minimum for both carbon and silicon in combination with the observable tendency of silicon clusters to have a spherical form, one can assume that processes similar to Stone–Wales rearrangement from polycyclic carbon structures to fullerene is also possible for silicon under certain conditions. Currently there is no common opinion on this question; however, in addition to the notes about direct syntheses of non-carbon fullerenes, it is possible to specify some new approaches.

The condensed analogues of the fullerenes have been produced in the well-crystallized hexagonal phases of Na–In–Z (Z represents Ni, Pd, Pt).<sup>6</sup> A typical molecule in this new class has the formula of Na<sub>96</sub>In<sub>97</sub>Z<sub>2</sub>, where Z can be nickel, palladium, or platinum. It consists of an In<sub>74</sub> cage surrounding a sodium cage which in turn encloses In<sub>10</sub>–Z units.

A new way of constructing non-carbon, fullerene-like curved molecular surfaces has been proposed by Harada et al.<sup>1a</sup> Following their initial suggestion, it is possible to utilize C<sub>60</sub> as the reactive core and to attach atoms of elements known to form strong carbide bonds onto the surface of C<sub>60</sub>. Particularly, ab initio calculations have shown that formation of the C<sub>60</sub>@Si<sub>60</sub> complex is energetically favorable.<sup>1b</sup>

In the present work we have extended these previous investigations through a uniform systematic study of the equilibrium geometries and electronic properties of all isovalent IV main group fullerene-like compounds: C<sub>60</sub>, Si<sub>60</sub>, Ge<sub>60</sub>, Sn<sub>60</sub>, and Pb<sub>60</sub> in order to provide the necessary data for further evaluation of new heavier analogs of the classical fullerene.

## Computational Method

The GAUSSIAN92/DFT<sup>26</sup> package was used for the ab initio SCF MO calculations at the Hartree–Fock and hybrid DFT levels. Lan11DZ, a computationally efficient basis set containing a pseudopotential for the core electron of Si, Ge, Sn, and Pb was employed.

The effect of electron correlation was estimated using the empirically parameterized Becke3LYP method.<sup>27–29</sup> These functionals implemented in the GAUSSIAN92 program are slightly different from the original formula suggested by Becke. Becke3LYP uses a combination of LYP<sup>30</sup> and the VWN<sup>31</sup> correlation functional instead of PW91. In addition, the effect of the basis set on the structure and properties of C<sub>60</sub> and Si<sub>60</sub> is examined at the STO-3G, Lan11DZ, and 6-31G(d) levels.

## Results and Discussion

Tables 1 and 2 summarize the optimized geometry and energy parameters for C<sub>60</sub>, Si<sub>60</sub>, Ge<sub>60</sub>, Sn<sub>60</sub>, and Pb<sub>60</sub> obtained at the Hartree–Fock and DFT levels.

**TABLE 1: Selected Structural and Energetic Parameters for the C<sub>60</sub>, Si<sub>60</sub>, Ge<sub>60</sub>, Sn<sub>60</sub>, and Pb<sub>60</sub> Compounds (HF/Lan11DZ Level)<sup>a</sup>**

	HF/Lan11DZ				
	C <sub>60</sub>	Si <sub>60</sub>	Ge <sub>60</sub>	Sn <sub>60</sub>	Pb <sub>60</sub>
R <sub>1</sub> distance	1.3797	2.1883	2.3143	2.6613	2.9184
Mulliken overlap population	0.3177	0.4957	0.4589	0.4354	0.2180
R <sub>2</sub> distance	1.4559	2.2656	2.3981	2.7503	2.9613
Mulliken overlap population	0.2738	0.3576	0.3369	0.3208	0.2092
bond alternation	0.0762	0.0773	0.0838	0.0890	0.0429
average diameter	7.080	11.091	11.737	13.473	14.601
total energy	-2271.09538	-224.81941	-218.44963	-195.64533	-200.81336
isolated atom energy	-37.59892	-3.61394	-3.53918	-3.17976	-3.28559
cohesive energy	-15.16018	-7.98301	-6.09883	-4.85973	-3.67796
HOMO-LUMO gap	0.2720	0.1610	0.1526	0.1322	0.0580

<sup>a</sup> All distances are in angstroms; energies and HOMO-LUMO gaps are in atomic units.

**TABLE 2: Selected Structural and Energetic Parameters for the C<sub>60</sub>, Si<sub>60</sub>, Ge<sub>60</sub>, Sn<sub>60</sub>, and Pb<sub>60</sub> Compounds (B3LYP/Lan11DZ Level)<sup>a</sup>**

	Becke3LYP/Lan11DZ				
	C <sub>60</sub>	Si <sub>60</sub>	Ge <sub>60</sub>	Sn <sub>60</sub>	Pb <sub>60</sub>
R <sub>1</sub> distance	1.4041	2.2196	2.3620	2.7232	2.9690
Mulliken overlap population	0.3530	0.4199	0.3531	0.3076	0.1721
R <sub>2</sub> distance	1.4638	2.2769	2.4259	2.7903	2.9821
Mulliken overlap population	0.3487	0.3254	0.2828	0.2539	0.1633
bond alternation	0.0596	0.0572	0.0638	0.0670	0.0131
average diameter	7.149	11.183	11.910	13.710	14.757
total energy	-2285.72151	-232.81672	-226.6558	-203.51826	-209.49898
isolated atom energy	-37.78697	-3.71926	-3.64561	-3.28343	-3.39247
cohesive energy	-18.50331	-9.66112	-7.91920	-6.51246	-5.95078
HOMO-LUMO gap	0.1038	0.0550	0.0364	0.0118	0.0113

<sup>a</sup> All distances are in angstroms; energies and HOMO-LUMO gaps are in atomic units.

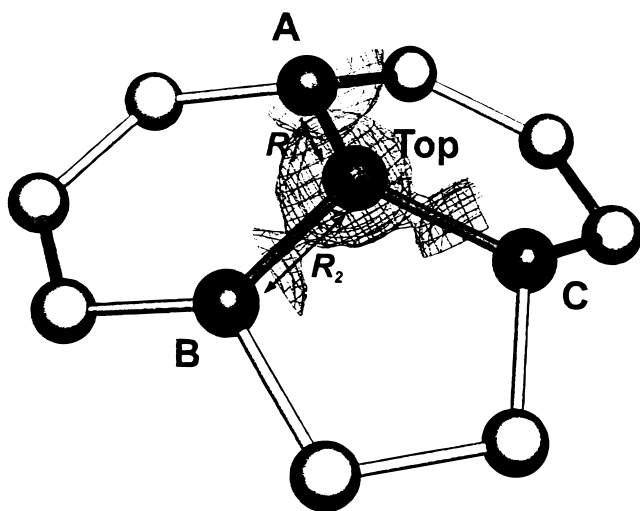


**Figure 1.** A fragment of fullerene structure in which the two types of bonds ( $R_1$ , double, and  $R_2$ , single) and corresponding electrostatic potential are depicted.

Like all closed geodesic structures, C<sub>60</sub> has the 12 pentagons that are required to transform a network into a spheroid. The remaining carbon atoms are configured as 20 hexagons to form the molecule's soccerball shape. Fullerenes follow the net closing formula postulated by Leonhard Euler. He states that for any polygon with  $n$  edges, at least one polyhedron can be constructed with 12 pentagons and  $(n - 20)/2$  hexagons.

In the case of the highly symmetric truncated icosahedral C<sub>60</sub>, it is necessary to determine only two independent geometric parameters, for example, the lengths of the bonds between the sixfold rings ( $R_1$ ) and the bonds sharing fivefold and sixfold rings ( $R_2$ ). In Figure 1 those two types of bonds are displayed along with the electrostatic potential of C<sub>60</sub>.

From a chemical point of view, bond alternation is an important feature of strained five-membered rings adjacent to benzene rings—the tendency to avoid forming double bonds in a pentagon ring.<sup>32</sup> The presence of double bonds shortens the bonds in the already-strained ring, producing the Mills–Nixon effect.<sup>33</sup>

It is of interest to study this tendency for the other molecules. Tables 1 and 2 show that absolute bond alternation increases from C<sub>60</sub> to Sn<sub>60</sub> and then significantly decrease for Pb<sub>60</sub>. The only prediction of 0.057 Å for Si<sub>60</sub> (B3LYP/Lan11DZ) does not follow this order (Figure 2a). In this case the difference between the bond length is smaller than that for C<sub>60</sub>, in contradiction with the previously obtained results<sup>2</sup> and our HF/Lan11DZ calculations. It is well known that the HF bond length differences tend to be overestimated as compared with experimental values.<sup>3</sup> The calculated HF/Lan11DZ level bond difference of 0.076 Å for C<sub>60</sub> compares favorably with the previous HF results but deviates from the experimental value of 0.05 Å.<sup>34</sup> However the B3LYP/Lan11DZ method for C<sub>60</sub> gives results which agree well with the experiments. Therefore, discrepancy in bond alternation for Si<sub>60</sub> requires closer investigation. We have calculated bond-length differences for C<sub>60</sub> and Si<sub>60</sub> using the HF/STO-3G, HF/Lan11DZ, HF/6-31G(d), and B3LYP/6-31G(d) levels. Tables 3 and 4 show that by using the extended basis sets the difference in bond lengths for Si<sub>60</sub> becomes smaller than for C<sub>60</sub>, as was established at the B3LYP/Lan11DZ level.

Another insight into the nature of these compounds can be obtained from examination of charge redistribution. The Mulliken overlap populations corresponding to the  $R_1$  and  $R_2$  bonds are reported in Tables 1 and 2. Mulliken charges are sensitive to the choice of basis set and can sometimes give unexpected results since the arbitrary division of overlap between atomic centers may be inappropriate.<sup>35,36</sup> On the other hand, a Mulliken-type analysis may be quite adequate for studying the relative

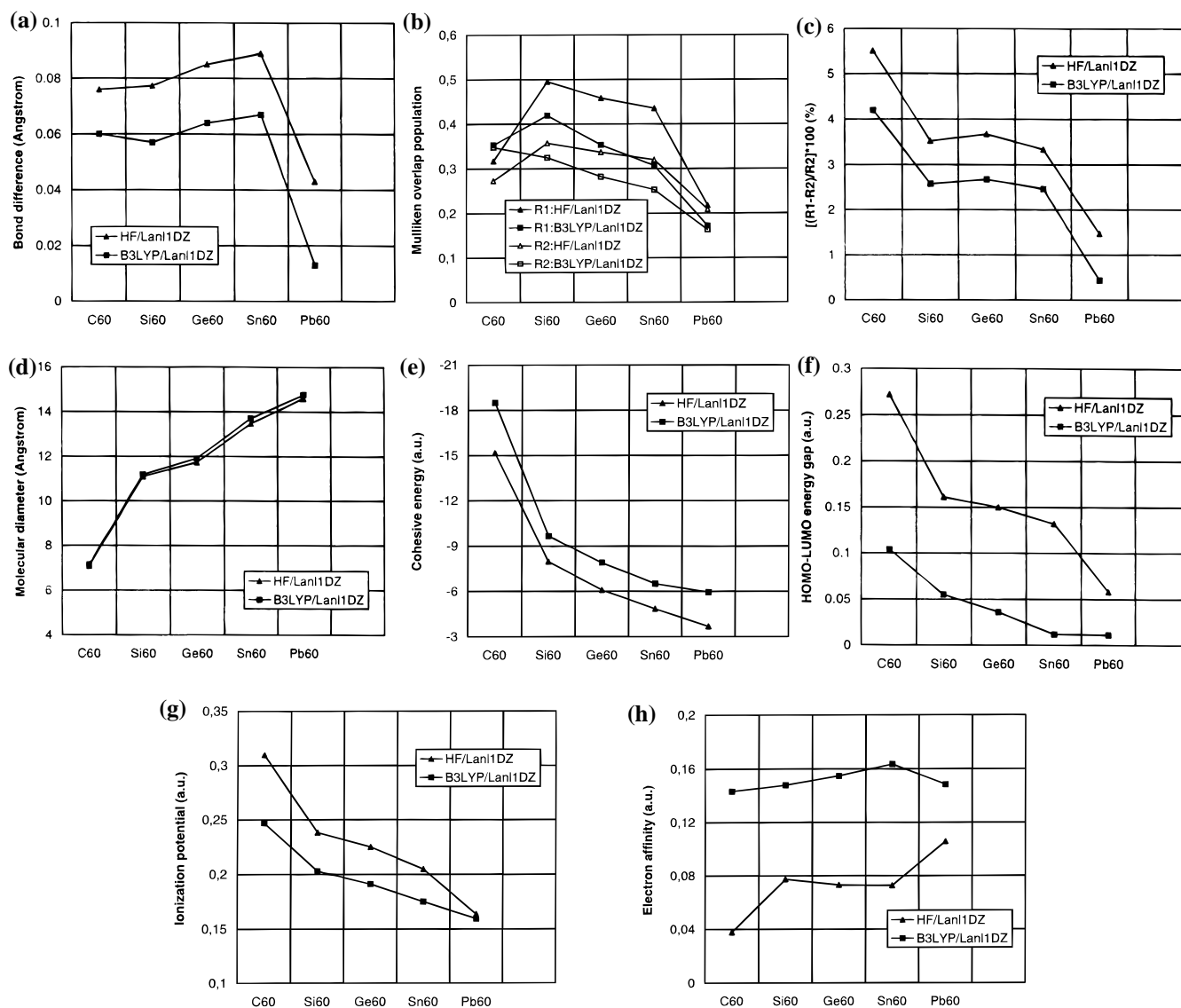


**Figure 2.** The dependencies of the structural parameters, and energetic and electronic properties of  $C_{60}$ ,  $Si_{60}$ ,  $Ge_{60}$ ,  $Sn_{60}$ , and  $Pb_{60}$  fullerene-like molecules (HF/Lan1DZ and B3LYP/Lan1DZ levels): (a) bond difference (Å) between the two types of bonds in the fullerene structure; (b) Mulliken overlap population of the double and single fullerene bonds; (c) relative bond alternation (%); (d) molecular diameter (Å); (e) cohesive energy (au); (f) HOMO–LUMO energy gap (au); and (g) ionization potential (au); and (h) electron affinity (au).

**TABLE 3: Selected Structural and Energetic Parameters for the  $C_{60}$  with the Different Basis Sets<sup>a</sup>**

	$C_{60}$				
	HF/STO-3G	HF/Lan1DZ	HF/6-31G(d)	B3LYP/Lan1DZ	B3LYP/6-31G(d)
$R_1$ distance	1.3760	1.3797	1.3728	1.4041	1.3953
Mulliken overlap population	0.5222	0.3177	0.5882	0.3530	0.5185
$R_2$ distance	1.4625	1.4559	1.4488	1.4638	1.4535
Mulliken overlap population	0.4361	0.2738	0.4547	0.3487	0.4492
bond alternation	0.0865	0.0762	0.0759	0.0596	0.0581
total energy	-2244.22124	-2271.09538	-2271.82698	-2285.72151	-2286.13713
isolated atom energy	-37.08958	-37.59892	-37.58827	-37.78697	-37.77446
cohesive energy	-18.84644	-15.16018	-16.53078	-18.50331	-19.66953
HOMO–LUMO gap	0.3179	0.2720	0.2722	0.1038	0.1013

<sup>a</sup> All distances are in angstroms; energies and HOMO–LUMO gaps are in atomic units.

trends as opposed to the absolute charges.<sup>37</sup> Figure 2b presents the Mulliken overlap populations of the single and double bonds for all fullerene-like complexes. Excluding the absolute difference between bond lengths, Mulliken analyses do not display any unusual features for  $Si_{60}$ .

Additionally, information about the bonding properties of the studied compounds can be obtained from the relative bond alternation calculated at the HF and B3LYP levels (Figure 2c).

With the HF approach, it is shown that these values for  $C_{60}$  are approximately four times larger than those obtained for  $Pb_{60}$ . However, the relative bond alternation for  $Si_{60}$ ,  $Ge_{60}$ , and  $Sn_{60}$  is rather similar, emphasizing the close values for their bond strength. The molecular diameters corresponding to increasing bond lengths are shown in Figure 2d.

The most important quantity for understanding the trends in the formation of fullerene-like molecules is the cohesive energy,



**TABLE 4: Selected Structural and Energetic Parameters for the Si<sub>60</sub> with the Different Basis Sets<sup>a</sup>**

	Si <sub>60</sub>				
	HF/STO-3G	HF/Lan1DZ	HF/6-31G(d)	B3LYP/Lan1DZ	B3LYP/6-31G(d) <sup>38</sup>
R <sub>1</sub> distance	2.0885	2.1883	2.2089	2.2196	2.2089
Mulliken overlap population	0.3901	0.4957	0.5362	0.4199	0.4379
R <sub>2</sub> distance	2.1686	2.2656	2.2836	2.2769	2.2836
Mulliken overlap population	0.3398	0.3576	0.3676	0.3254	0.3699
bond alternation	0.0801	0.0773	0.0746	0.0572	0.0746
total energy	-17135.92164	-224.81941	-17334.3808	-232.81672	-17369.45958
isolated atom energy	-285.38397	-3.61394	-288.76918	-3.71926	-289.32689
cohesive energy	-12.88344	-7.98301	-8.22999	-9.66112	-9.84618
HOMO–LUMO gap	0.2010	0.1610	0.1551	0.0550	0.0221

<sup>a</sup> All distances are in angstroms; energies and HOMO–LUMO gaps are in atomic units.

defined as the difference of the total molecular energy and the sum of the energies of the isolated atoms. Figure 2e shows the cohesive energy curves (the HF and B3LYP approaches) for C<sub>60</sub>, Si<sub>60</sub>, Ge<sub>60</sub>, Sn<sub>60</sub>, and Pb<sub>60</sub>. As expected, the cohesive energy decreases considerably from C<sub>60</sub> to Pb<sub>60</sub>. The maximum HF value of -15.160 au (-18.503 au, B3LYP) corresponds to C<sub>60</sub>, and the minimum value -3.677 au (-5.950 au) corresponds to Pb<sub>60</sub>. The other values lie in between and are relatively close to each other.

The electronic energy level orders and degeneracy around energy gap for C<sub>60</sub> are in good agreement with the available results.<sup>7</sup> The highest-occupied state of the C<sub>60</sub> cluster is the fivefold degenerated h<sub>u</sub> state, and the energy gap between h<sub>u</sub> and the lowest unoccupied threefold degenerated t<sub>1u</sub> state is about 0.27 au.

Changes of the HOMO–LUMO energy gaps corresponding to the different fullerene-like compounds are shown in Figure 2f. The HF and B3LYP methods predict the energies of these two molecular orbitals rather differently, although there is excellent agreement when the energy trend through the series is considered. It should be noticed that the energy of HOMO changes the most along the series and that all orbital energies of LUMO are negative.

It is of interest that the trends displayed in the plots in Figure 2c,e,f are in the same direction. Comparison of the HF and B3LYP results indicates that inclusion of electron correlation does not considerably change the geometric dependencies (except for the bond difference for Si<sub>60</sub> considered above). Similar results are also obtained for the cohesive energy and HOMO–LUMO energy gaps.

On the basis of the molecular orbital energies, all the non-carbon clusters considered in this work seem to be better electron donors and better electron acceptors than C<sub>60</sub>. They also possess lower electronically excited states and therefore should display enhanced nonlinear optical properties. Interestingly, the energy gap, which plays a direct role in the determination of the metallic behavior of the system, changes negligibly when we consider the HF level data for the semiconducting Si and Ge or the metal Sn.

Since a detailed investigation of these problems is beyond the framework of our paper, we shall therefore present only the values of the ionization potential (Figure 2g) and the electron affinity (Figure 2h) which are a direct product (using Koopman's theorem) of our calculations.

An examination of the energy levels computed by the different methods indicates also the small values of the HOMO–LUMO gap for the presented structures obtained from the DFT method. Quite surprisingly, the Becke3LYP combination of DFT functionals leads to the worst representation of the electronic spectra, underestimating HOMO–LUMO energy gaps and the LUMO-1 levels and yielding a poor description of the energy-

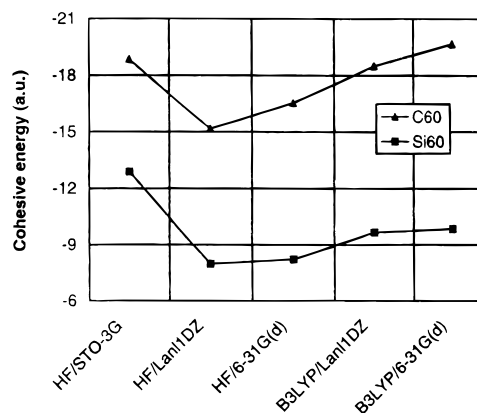


**Figure 3.** Basis set influence on the cohesive energy (au) of C<sub>60</sub>, Si<sub>60</sub>, Ge<sub>60</sub>, Sn<sub>60</sub>, and Pb<sub>60</sub> (the HF and B3LYP approaches).

level order and degeneracy. These results are not in line with the calculations of the geometric parameters and cohesive energy where the Becke3LYP and HF approaches were found nearly equivalent.

**Basis Set Influence.** We have tested several different basis sets—STO-3G (HF level), Lan1DZ, and 6-31G(d) (both at the HF and B3LYP levels)—in order to monitor the convergence of our results with increasing basis size (Tables 3 and 4).

The values of the cohesive energy for C<sub>60</sub> and Si<sub>60</sub> are given in Figure 3. It is notable that although the cohesive energy changes depending on the chosen basis sets and computational methods, the relative tendencies are reproduced well at all tested levels.

Tables 3 and 4 show that the most important structural trends are also well reproduced by both the HF and the hybrid DFT level methods. The only exception is the values of bond differences for Si<sub>60</sub> discussed above. In the case of Ge<sub>60</sub>, additional geometry optimizations were performed using the Lan1DZ basis set augmented by a set of d-polarization functions ( $\varphi = 0.246$ ) at both HF and DFT levels. The optimized molecular parameters (HF:  $R_1 = 2.3138$ ,  $R_2 = 2.3982$ ,  $E = -219.20632$ ; DFT:  $R_1 = 2.3577$ ,  $R_2 = 2.4133$ ,  $E = -227.17367$ ) are slightly shorter than those obtained using the standard Lan1DZ basis set.

Finally, basis set effects were tested on the HOMO–LUMO energies. Using the B3LYP method, a much smaller energy gap is obtained (Figure 4), but again, this should have only a small effect on the relative trends. Therefore, Tables 3 and 4 indicate that for the studied species the Lan1DZ basis set is a well-balanced choice from the point of view of accuracy of the results and computational efficiency.

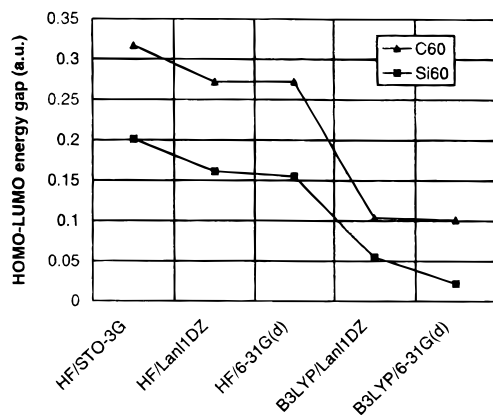


**Figure 4.** Comparison of the HOMO–LUMO energy gaps (au) of C<sub>60</sub>, Si<sub>60</sub>, Ge<sub>60</sub>, Sn<sub>60</sub>, and Pb<sub>60</sub> using different basis sets (the HF and B3LYP approaches).

## Conclusions

This paper presents the results of a comprehensive investigation of the IV main group fullerene-like compounds X<sub>60</sub> (X = C, Si, Ge, Sn, and Pb) by ab initio molecular modeling. Fullerene-like structures for all considered compounds are stationary points on the respective potential energy surfaces, and all X<sub>60</sub> species are stable toward dissociation into 60 X atoms. Our calculations confirmed the possibility of the existence of these species. We have for the first time provided systematic high-level data for the equilibrium geometries, cohesive energies, and electronic properties for all of these species. The values of the relative bond alternation, cohesive energy, HOMO–LUMO gap, and the ionization potential of the molecules decrease monotonically in going down the IVth group from C<sub>60</sub> to Pb<sub>60</sub>. The dependencies of the absolute bond difference, Mulliken overlap population, and the electron affinity have a more complicated character.

As expected, for Ge<sub>60</sub> the obtained data is rather similar to that for Si<sub>60</sub>, but it was also found that the molecular parameters for Sn<sub>60</sub> are close to the appropriate values both for Si<sub>60</sub> and Ge<sub>60</sub>. In light of the method offered by Harada et al.,<sup>1a</sup> the given circumstance opens the opportunity for synthesis of new metal-coated fullerenes like Si<sub>60</sub>@Sn<sub>60</sub> with rather unusual properties, which is interesting both from chemical and nanotechnological points of view.

**Acknowledgments.** This work was facilitated by NSF grant OSR-9452857 and the Army High Performance Computing Research Center under the auspices of the Department of the Army, Army Research Laboratory cooperative agreement number DAAH04-95-2-0003/contract number DAAH04-95-C-0008, the content of which does not necessarily reflect the position or the policy of the government, and no official endorsement should be inferred.

## References and Notes

(1) (a) Harada, M.; Osawa, S.; Osawa, E.; Jemmis, E. D. *Chem. Lett.* **1994**, 1037. (b) Jemmis, D. E.; Leszczynski, J.; Osawa, E. *Fullerene Sci. Technol.* **1998**, 6, 271.

(2) Piqueras, M. C.; Crespo, R.; Orti, E.; Tomas, F. *Chem. Phys. Lett.* **1993**, 213, 509.

(3) Nagase, S.; Kobayashi, K. *Chem. Phys. Lett.* **1991**, 187, 291.

(4) Jemmis, E. D.; Kiran, B. In *Computational Chemistry: Reviews of Current Trends*, Vol. 1; Leszczynski, J., Ed.; World Scientific: Singapore, 1996; p 175.

(5) Nesper, R. *Angew. Chem. Int. Ed. Engl.* **1994**, 33, 843.

(6) Sevov, S.; Corbett, J. *Science* **1993**, 262, 880.

(7) De Proft, F.; Van Alsenoy, C.; Geerlings, P. *J. Phys. Chem.* **1996**, 100, 7440.

(8) Nagase, S. *Polyhedron* **1991**, 10, 1299.

(9) Nagase, S. *Pure Appl. Chem.* **1993**, 65, 675.

(10) Smalley, R. E. In *Comparison of ab Initio Quantum Chemistry with Experiment for Small Molecules*, Bartlett, R. J., Ed.; D. Reidel Publishing Company: Boston, 1985; p 53.

(11) Bloomfield, L. A.; Geusic, M. E.; Freeman, R. R.; Brown, W. L. *Chem. Phys. Lett.* **1985**, 121, 3.

(12) Elkind, J. E.; Alford, J. M.; Weiss, F. D.; Laaksonen, R. T.; Smalley, R. E. *J. Chem. Phys.* **1987**, 87, 2397.

(13) Jarrold, M. F.; Constant, V. A. *Phys. Rev. Lett.* **1991**, 67, 2994.

(14) Rinnen, K. D.; Mandich, M. L. *Phys. Rev. Lett.* **1992**, 69, 1823.

(15) Haufler, R. E.; Chai, Y.; Chibante, L. P. F.; Conceicao, J.; Jin, C.; Wang, L.-S.; Maruyama, S.; Smalley, R. E. *Mat. Res. Soc. Symp. Proc.* **1991**, 206, 627.

(16) Maruyama, S.; Yamaguchi, Y. *Therm. Sci. Engng.* **1995**, 3, 105.

(17) Robertson, D. H.; Brenner, D. W.; White, C. T. *J. Phys. Chem.* **1992**, 96, 6133.

(18) Dravid, V. P.; Lin, X.; Wang, Y.; Wang, X. K.; Yee, A.; Ketterson, J. B.; Chang, R. P. H. *Science* **1993**, 259, 1601.

(19) Heath, J. R. *Fullerenes*; Hammand, G. S., Kuck, V. J., Eds.; American Chemical Society: Washington, D. C., 1992; pp 1–23.

(20) Hunter, J. M.; Fye, J. L.; Roskamp, E. L.; Jarrold, M. F. *J. Phys. Chem.* **1994**, 98, 1810.

(21) Smalley, R. E.; Colbert, D. T. In *Proceedings from NATO Advanced Research Workshop: Modular Chemistry*; Michl, J., Ed.; Kluwer Academic Publishers: 1997.

(22) Hagelberg, F.; Leszczynski, J.; Murashov, V. *THEOCHEM* **1998**, 454, 209.

(23) Jackson, K. A. *Abstracts of the 1995 March Meeting of the American Physics Society*, March 20–24, 1995; San Jose, CA; B26.01.

(24) Schulman, J. M.; Disch, R. L.; Miller, M. A.; Peck, R. C. *Chem. Phys. Lett.* **1987**, 141, 45.

(25) Gong, X. G.; Zheng, Q. Q. *Abstracts of the 1996 March Meeting of the American Physics Society*, March 20–24, 1996, St. Louis, MO; G23.11.

(26) Frisch, M. J.; Trucks, G. W.; Schlegel, H. B.; Gill, P. M. W.; Johnson, B. G.; Wong, M. W.; Foresman, J. B.; Robb, M. A.; Head-Gordon, M.; Replogle, E. S.; Gomperts, R.; Andres, J. L.; Raghavachari, K.; Binkley, J. S.; Gonzalez, C.; Martin, R. L.; Fox, D. J.; Defrees, D. J.; Baker, J.; Stewart, J. J. P.; Pople, J. A. *Gaussian 92/DFT, Revision G.4*; Gaussian, Inc.: Pittsburgh, PA, 1993.

(27) Becke, A. D. *Phys. Rev. A* **1988**, 38, 3098.

(28) Stevens, P. J.; Devlin, F. J.; Chabalowski, C. F.; Frisch, M. J. *J. Phys. Chem.* **1994**, 98, 11623.

(29) Pavlov, M.; Siegbahn, P. E. M.; Sandstrom, M. *J. Phys. Chem.* **1998**, 102, 219.

(30) Lee, C.; Yang, W.; Parr, R. G. *Phys. Rev. B* **1988**, 37, 785.

(31) Vosko, S. H.; Wilk, L.; Nusair, M. C. *J. Phys.* **1980**, 58, 1200.

(32) Taylor, R.; Walton, D. R. M. *Nature* **1993**, 363, 685.

(33) Mills, W. H.; Nixon, I. J. *J. Chem. Soc.* **1930**, 2510.

(34) Yannoni, C. S.; Bernier, P. P.; Bethune, D. S.; Meijer, G.; Salem, J. R. *J. Am. Chem. Soc.* **1991**, 113, 3190.

(35) Orlova, G.; Scheiner, S. *J. Phys. Chem. A* **1998**, 102, 260.

(36) Cioslowski, J.; Surjan, P. R. *THEOCHEM* **1992**, 255, 9.

(37) McKee, M. L. *J. Am. Chem. Soc.* **1993**, 115, 2818.

(38) This is the result of the single-point B3LYP/6-31G(d) calculation on the HF/6-31G(d) optimized structure.